

Cite this article as: Zeng Bo, Xie Zhiqiang, Li Qiang, et al. Residual Stress Relaxation of 2A02 Blade Forging Under Electromagnetic Coupling Energy[J]. Rare Metal Materials and Engineering, 2023, 52(12): 4055-4064. DOI: 10.12442/j.issn.1002-185X.20230281.

ARTICLE

# Residual Stress Relaxation of 2A02 Blade Forging Under Electromagnetic Coupling Energy

Zeng Bo<sup>1,2</sup>, Xie Zhiqiang<sup>3</sup>, Li Qiang<sup>1,2</sup>, Wang Jie<sup>1,2</sup>, Huang Kunlan<sup>1,2</sup>, Yu Hang<sup>1,2</sup>

<sup>1</sup> School of Mechanical Engineering, Sichuan University, Chengdu 610065, China; <sup>2</sup> Yibin Institute, Sichuan University, Yibin 644005, China;

<sup>3</sup> AECC AERO Science and Technology Co., Ltd, Chengdu 610599, China

**Abstract:** A novel method of electromagnetic coupling treatment (EMCT) was proposed to control the residual stress of 2A02 aluminum alloy blade forging in compressor, aiming at solving the industrial problem of machining deformation of large-size thin-wall parts due to residual stress releasing. The effects of electric and magnetic field treatment on the residual stress and mechanical properties of forgings were studied. The microstructure was analyzed by quasi-in-situ EBSD. The results show that compared with a single physical field, the EMCT has the most significant relaxation effect on residual stress. When the magnetic field intensity is 1.5 T and the electric field intensity is 750 V/m, the maximum reduction of residual stress of blade forging is 53%. EMCT can improve the plasticity of aluminum alloy without damaging the strength. Under the above parameters, the elongation is increased by 14.3% and the resistance is decreased by 4.9%. EBSD quasi-in-situ analysis shows that after EMCT, the geometric dislocation density of forgings is reduced by 58.2%, the small-angle grain boundaries are reduced, the plug dislocations are dispersed and annihilated, the local strain is reduced, and the macroscopic stress is relaxed.

**Key words:** aluminum alloy forgings; residual stress; electromagnetic coupling treatment; dislocation annihilation

The processing deformation of large-size thin-walled parts is an industrial problem in the field of aviation manufacturing<sup>[1]</sup>. The warping and torsional deformation of parts after processing seriously affect the processing efficiency and subsequent assembly quality<sup>[2]</sup>. In addition, the processing deformation problem is characterized by strong randomness and large dispersion, which greatly increase the difficulty of aviation manufacturing and are difficult to prevent<sup>[3]</sup>. The residual stress in the workpiece is considered to be one of the main causes for machining deformation<sup>[4-5]</sup>. Therefore, in order to alleviate the processing deformation caused by stress release, residual stress regulation should be carried out on the workpiece before or during processing. The existing stress relaxation methods mainly include heat treatment<sup>[6]</sup>, natural aging<sup>[7-8]</sup>, mechanical vibration<sup>[9-10]</sup>, etc, which have some problems such as high energy consumption, long period and poor effect. It is a new technology different from traditional processing methods to use electromagnetic field to release stress and to adjust performance of

materials<sup>[11]</sup>. Cai et al<sup>[12]</sup> conducted pulse magnetic processing on forged medium carbon steel, and found that magnetostriction effect can bring stress reduction, and that dislocation movement occurs in magnetic field. Song et al<sup>[13]</sup> conducted low-frequency alternating magnetic field treatment on welded parts of alloy steel, and the average stress of the sample was reduced by more than 20%. They proposed that dislocation movement accompanied with magnetoplastic deformation is the fundamental cause of stress release. Shao<sup>[14]</sup> and Zhang<sup>[15]</sup> adopted pulsed magnetic field with intensity of 1 T to treat low-alloy steel, and found that the residual stress of the sample is decreased by 14%, and they pointed out that the stress release is related to the transition of magnetic domain in the samples. Yan et al<sup>[16]</sup> adopted pulsed magnetic field to treat rolled magnesium alloy sheet and found that the residual stress is reduced by 30.3% at most, believing that Joule thermal effect brought by pulsed magnetic field is conducive to stress elimination. Xiang et al<sup>[17]</sup> found that the electrical pulse treatment can significantly reduce the quenching stress

Received date: May 11, 2023

Foundation item: National Natural Science Foundation of China (51705348); AECC Independent Innovation Fund (ZZCX-2021-031, ZZCX-2022-036)

Corresponding author: Huang Kunlan, Ph. D., Associate Professor, School of Mechanical Engineering, Sichuan University, Chengdu 610065, P. R. China, E-mail: huangkunlan@scu.edu.cn

Copyright © 2023, Northwest Institute for Nonferrous Metal Research. Published by Science Press. All rights reserved.

of metal materials, and the reason is that the drifting electron energy promotes dislocation slip.

Electromagnetic coupling treatment is to strengthen metal parts after coupling pulsed electric field and magnetic field, and to make the thermal and non-thermal effects of electric field and magnetic field jointly act on materials, so as to realize material modification by regulating the microstructure defects of materials. It has the advantages of short process time and environmental friendliness, without change in the morphology of parts and composition<sup>[18-19]</sup>. Zhong<sup>[20]</sup> proved that electromagnetic coupling treatment can reduce the stress of P10 tool by 65%. According to the study of Sun<sup>[21]</sup>, the micro-vibration effect caused by electromagnetic pulse can adjust the overall residual stress distribution of the sample and repair the microscopic defects. Existing studies have shown that electromagnetic field treatment can adjust the stress of materials, but most of the results are focused on the treatment and evaluation of experimental samples, and there are few reports on the whole research of parts.

In the present study, 2A02 blade forgings were taken as the object, electromagnetic field method was adopted to conduct stress relaxation treatment on blades, the relaxation effect was evaluated through the value and state of blade residual stress, and the influence of electromagnetic field treatment on the conductive and mechanical properties of blade materials was characterized. Finally, through the EBSD analysis of material microstructure, the mechanism of blade stress relaxation under the action of electromagnetic coupling energy was explained from the microscopic point of view.

## 1 Experiment

The research object of this experiment was compressor aluminum alloy blade forging, the size was 120 mm×110 mm×480 mm and the state was solution aged. The blade material was 2A02 aluminum alloy, and the composition is shown in Table 1. The schematic diagram of electromagnetic field processing for blades is shown in Fig. 1. Both ends of the blade were connected with copper electrodes for conducting electricity, and the whole blade was placed in the coil cavity. When a voltage was applied at both ends of the copper electrode, an electric field was formed. The pulsed current flowing through the coil will generate a pulsed magnetic field inside the cavity. PLC was used to control the electrode and coil line off, which can form different states of space field (single electric field, single magnetic field, electromagnetic coupling field) in the cavity, so as to achieve different treatments of the blade: electric current treatment (CT), magnetic treatment (MT), electromagnetic coupling treatment (EMCT). The experimental parameters of this group were designed as shown in Table 2. Three blade forging billets were used in each group of experiments to reduce accidental errors.

**Table 1** Chemical composition of 2A02 alloys (wt%)

Cu	Mg	Mn	Si	Fe	Zn	Ti	Al
2.92	2.21	0.59	0.29	0.33	0.11	0.15	Bal.

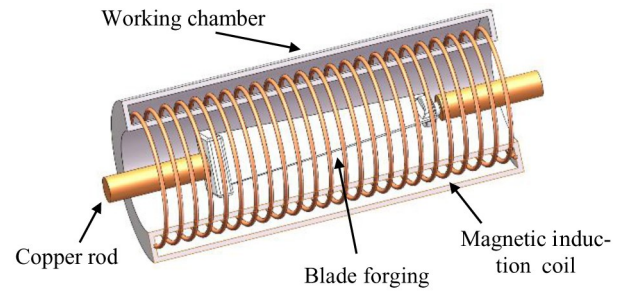


**Fig.1** Schematic diagram of electromagnetic field treatment for blade forgings

**Table 2** Experimental parameters for different treatments of blades

Group	Electric field intensity/ $V \cdot m^{-1}$	Magnetic field intensity/T	Processing time /s
CT	750	0	200
MT	0	1.5	200
EMCT	750	1.5	200

XL-640 X-ray diffractometer was used to measure residual stress distribution at blade calibration points according to GB/T 7704-2017. The calibration points are shown in Fig. 2. According to the machining deformation characteristics of the blade, five test points were selected in the leaf basin and the back of the blade, the test was repeated 3 times at each point, and the average value was taken as the stress value of the point. The measurement process adopted the fixed tilt method, the ray source was Cu-K $\alpha$ , the tube voltage was 25 kV, the tube current was 5 mA, the diameter of the collimator was 1 mm, and the fixed peak method was the finite cross correlation method. Before the blade was treated with electromagnetic field, the first round of stress test was carried out. The measured results were taken as the initial residual stress. After the electromagnetic field treatment, the second round of stress test was carried out at the same point, so as to

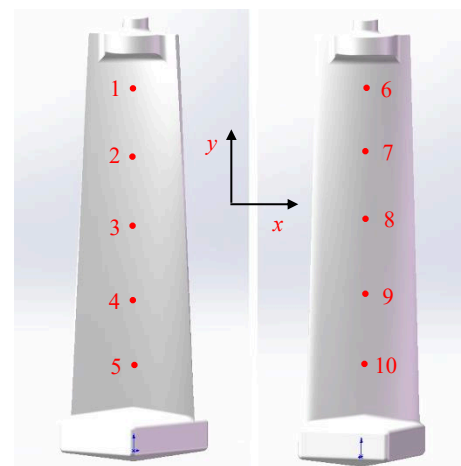


**Fig.2** Diagram of residual stress test points

evaluate the degree of stress relaxation. Samples were cut and sampled in the same batch of forgings, and the samples were subjected to electromagnetic field treatment with the same parameters, and then performance test was carried out.

Tensile samples were prepared according to GB/T 228-2002, and the surface roughness did not exceed  $R_a=0.8$ . The size of the tensile sample is follows:  $a_0=3$  mm,  $b_0=12.5$  mm,  $L_0=50$  mm,  $L_c=54$  mm,  $R=20$  mm,  $L_t=112.3$  mm. ETM305D universal testing machine was used for tensile test at room temperature. The standard distance was 50 mm and the loading rate was 2 mm/min. The tensile fracture was observed and analyzed by JSM-7500F high resolution scanning electron microscope and EDS X-Max Oxford spectrometer. The equipment used to measure the resistance of sample at room temperature was B2985A electrometer, the test current was 5 mA, the accuracy was  $1 \times 10^{-6} \Omega$ , the sample size was  $100 \text{ mm} \times 10 \text{ mm} \times 2 \text{ mm}$ , and each sample was measured three times to take the mean. The sample size for microstructure analysis was  $10 \text{ mm} \times 10 \text{ mm} \times 2 \text{ mm}$ , and they were polished with 500#, 1000#, 1500#, 2000# silicon carbide sandpaper, then subjected to mechanical polishing with diamond polishing agent, and electrolytic polishing, using electrolyte consisting of 10%  $\text{HClO}_4+90\%$  ethanol, at 30 V for 25 s. The microstructures of the samples were observed by electron back scattering diffraction (EBSD) method before treatment, and then characterized by in situ observation with the same method after treatment. The working voltage of the detector was 20 kV and the scanning step was 3.3  $\mu\text{m}$ . The test data were analyzed by HKL Channel 5 software.

## 2 Results and Discussion

### 2.1 Residual stress

The residual stress of blade forgings was measured before

and after electromagnetic field treatment. The residual stress data of blades treated by magnetic field, electric field and electromagnetic coupling treatment are shown in Table 3, Table 4 and Table 5, respectively. MT-1 represents the first test point,  $\sigma_x$  represents the measured residual stress in the  $x$  direction before the magnetic field is applied, and  $\sigma_x'$  represents the measured residual stress in the  $x$  direction after the electromagnetic field is applied. The negative stress value represents the compressive stress state, and the positive one represents the tensile stress state. In the fourth column,  $\Delta\sigma_x$  is the calculated value (the change in the absolute value of residual stress), and the negative value indicates that the point changes from a high stress level to a lower stress level after treatment. In the fifth column, the change rate of absolute value reflects the change of stress value. Negative value indicates that the magnitude of residual stress decreases; otherwise, it increases. The changing trend of stress amplitude is shown by the arrow in the sixth column.

Fig. 3 shows the change of residual stress distribution of blade forgings before and after electromagnetic field treatment. It demonstrates that the initial residual stress states of different test points in blade forging differ greatly, and there are differences in the states of tensile stress and compressive stress as well as stress levels. After the treatment of single electric field, single magnetic field and electromagnetic coupling, the stress values of most points are reduced to varying degrees, which mainly includes the reduction of tensile stress (such as MT-1, MT-5) and compressive stress (such as MT-3, MT-4). As far as blade processing is concerned, lower residual stress level is helpful to alleviate dimensional aberration in machining<sup>[2]</sup>. Therefore, it is of key significance to realize stress relaxation of blade forging by electromagnetic field processing to alleviate blade machining deformation.

Table 3 Residual stress test results of single blade before and after MT

Point	Before treatment, $\sigma_x/\text{MPa}$	After treatment, $\sigma_x'/\text{MPa}$	Absolute value change, $\Delta\sigma_x= \sigma_x'  -  \sigma_x /\text{MPa}$	Ratio of absolute change, $ \sigma_x /\%$	Stress amplitude change	Before treatment, $\sigma_y/\text{MPa}$	After treatment, $\sigma_y'/\text{MPa}$	Absolute value change, $\Delta\sigma_y= \sigma_y'  -  \sigma_y /\text{MPa}$	Ratio of absolute change, $ \sigma_y /\%$	Stress amplitude change
MT-1	298	197	-101	-33.9	↓	107	-121	14	13.1	↑
MT-2	34	89	55	161.8	↑	125	136	11	8.8	↑
MT-3	-514	-346	-168	-32.7	↓	314	217	-97	-30.9	↓
MT-4	-347	-241	-106	-30.5	↓	304	248	-56	-18.4	↓
MT-5	170	109	-61	-35.9	↓	339	261	-78	-23.0	↓
MT-6	247	-208	-39	-15.8	↓	-96	-53	-43	-44.8	↓
MT-7	191	188	-3	-1.6	↓	-237	-169	-68	-28.7	↓
MT-8	283	233	-50	-17.7	↓	-171	-142	-29	-17.0	↓
MT-9	-96	-77	-19	-19.8	↓	192	126	-66	-34.4	↓
MT-10	132	112	-20	-15.2	↓	188	139	-49	-26.1	↓
Deviation, $D$	266.02	196.92	-	-		223.57	172.22	-	-	

**Table 4 Residual stress test results of single blade before and after CT**

Point	Before treatment, $\sigma_x$ /MPa	After treatment, $\sigma_x'$ /MPa	Absolute value change, $\Delta\sigma_x =  \sigma_x' - \sigma_x $ /MPa	Ratio of absolute change, $\Delta\sigma_x'/ \sigma_x $ %	Stress amplitude change	Before treatment, $\sigma_y$ /MPa	After treatment, $\sigma_y'$ /MPa	Absolute value change, $\Delta\sigma_y =  \sigma_y' - \sigma_y $ /MPa	Ratio of absolute change, $\Delta\sigma_y'/ \sigma_y $ %	Stress amplitude change
CT-1	281	220	-61	-21.7	↓	95	62	-33	-34.7	↓
CT-2	102	83	-19	-18.6	↓	105	-78	-27	-25.7	↓
CT-3	194	141	-53	-27.3	↓	200	71	-129	-64.5	↓
CT-4	-318	-197	-121	-38.1	↓	341	217	-124	-36.4	↓
CT-5	-256	-196	-60	-23.4	↓	180	-147	-33	-18.3	↓
CT-6	192	-201	9	4.7	↑	-88	-92	4	4.5	↑
CT-7	99	-61	-38	-38.4	↓	-244	-175	-69	-28.3	↓
CT-8	364	199	-165	-45.3	↓	-263	-167	-96	-36.5	↓
CT-9	-199	-101	-98	-49.2	↓	117	-143	26	22.2	↑
CT-10	76	54	-22	-28.9	↓	-302	-188	-114	-37.7	↓
Deviation, $D$	227.64	157.87	-	-		212.15	143.68	-	-	

**Table 5 Residual stress test results of single blade before and after EMCT**

Point	Before treatment, $\sigma_x$ /MPa	After treatment, $\sigma_x'$ /MPa	Absolute value change, $\Delta\sigma_x =  \sigma_x' - \sigma_x $ /MPa	Ratio of absolute change, $\Delta\sigma_x'/ \sigma_x $ %	Stress amplitude change	Before treatment, $\sigma_y$ /MPa	After treatment, $\sigma_y'$ /MPa	Absolute value change, $\Delta\sigma_y =  \sigma_y' - \sigma_y $ /MPa	Ratio of absolute change, $\Delta\sigma_y'/ \sigma_y $ %	Stress amplitude change
EMCT-1	207	78	-129	-62.3	↓	74	-35	-39	-52.7	↓
EMCT-2	120	-57	-63	-52.5	↓	97	151	54	55.7	↑
EMCT-3	-191	-94	-97	-50.8	↓	295	154	-141	-47.8	↓
EMCT-4	-377	-165	-212	-56.2	↓	216	113	-103	-47.7	↓
EMCT-5	129	67	-62	-48.1	↓	171	142	-29	-17.0	↓
EMCT-6	56	35	-21	-37.5	↓	-334	-102	-232	-69.5	↓
EMCT-7	183	101	-82	-44.8	↓	-185	-58	-127	-68.6	↓
EMCT-8	-241	-93	-148	-61.4	↓	382	167	-215	-56.3	↓
EMCT-9	318	124	-194	-61.0	↓	164	-65	-229	-139.6	↓
EMCT-10	102	131	29	28.4	↑	281	116	-165	-58.7	↓
Deviation, $D$	214.18	101.24	-	-		239.87	118.33	-	-	

The stress level in the forgings should be as low as possible in terms of relaxation of residual stress to alleviate machining deformation. In order to evaluate the effect of different processes on blade stress regulation, index  $D$  was introduced by analogy with sample standard deviation, as shown in Eq.(1).

$$D = \sqrt{\frac{1}{n} \sum_{i=1}^n (\sigma_i - 0)^2} \quad (1)$$

where  $n$  is the number of test points,  $i$  represents the  $i$ th test

point, and  $\sigma_i$  is the stress value of the corresponding point.

Therefore, index  $D$  represents the dispersion of the column data with respect to stress value 0. The lower the  $D$  value, the better the stress towards 0 of the data, that is, the greater the stress relaxation range, the better the stress distribution uniformity. It can be seen from the table that after electromagnetic field treatment, the  $D$  value of each test point decreases significantly. The ratio of  $D$  value after and before

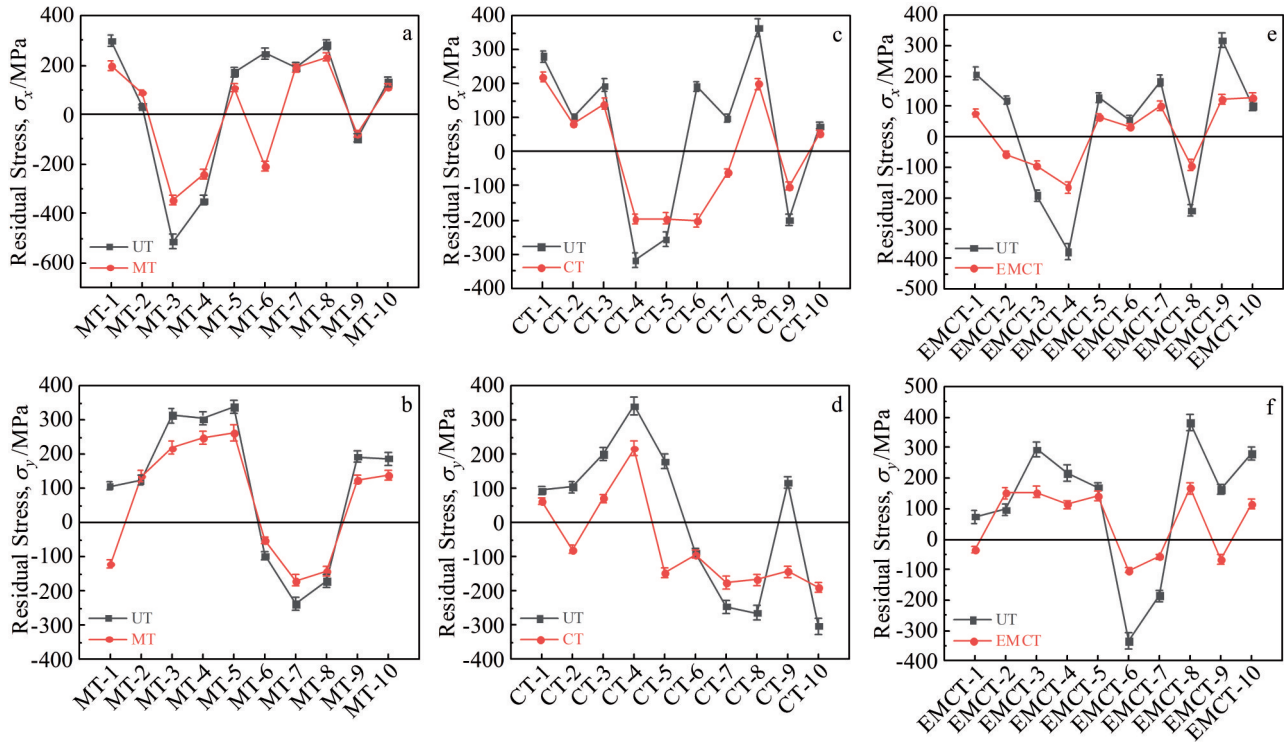


Fig.3 Changes of blade residual stress before (Untreated, UT) and after electromagnetic field treatment: (a) MT, x direction; (b) MT, y direction; (c) CT, x direction; (d) CT, y direction; (e) EMCT, x direction; (f) EMCT, y direction

treatment was calculated to evaluate the degree of stress relaxation caused by different processes, as shown in Table 6. It can be seen that the EMCT group has the smallest value, that is, after the electromagnetic coupling treatment, the residual stress relaxation effect of blade forging is the most obvious, and the overall stress level of the test point is only 47% of the initial state, that is, the reduction is 53%. In both compressive and tensile stress states, the stress level approaches to 0.

In addition, it is also found that the stress level of some test points is not only reduced, but also changes from tensile stress state to compressive stress state, such as the x-stress of MT-6 and y-stress of CT-5. The reduction of the peak value of residual stress and the uniformity of stress distribution play an active role in alleviating the size aberration and improving the yield of parts. The transition from tensile stress to compressive stress state helps to restrain crack propagation and improve the fatigue life of blade<sup>[22]</sup>.

**2.2 Strength and plasticity**

Tensile experiments at room temperature were carried out on original samples and samples treated with electromagnetic fields in different states, and the results are shown in Fig.4 and Fig.5. Fig.4 is the stress-strain curve.

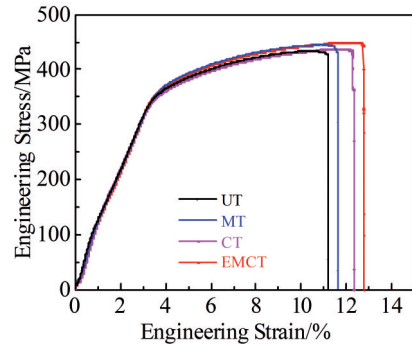


Fig.4 Stress-strain curves of original samples and samples treated with electromagnetic fields

It can be seen that there is no obvious yield phenomenon for all samples, and the stages of elastic deformation and plastic deformation are almost the same. The stress limit fluctuation of the samples is small, and the strain limit has obvious difference. Fig. 5 shows the comparison of tensile strength and elongation. It can be seen that neither single electric field, single magnetic field nor electromagnetic coupling treatment has an obvious effect on the tensile strength of the material, which is basically maintained at about 430 MPa. The elongation of the original sample is 11.2%, and increases to 11.6% and 12.3% after single magnetic field and single electric field treatment, respectively. After electromagnetic coupling treatment, the elongation is increased to 12.8%, with an increase of 14.3%. It can be seen that the external field treatment can improve the plasticity of 2A02 aluminum alloy to a certain extent, and the

**Table 6 Relaxation effect of different processes on residual stress**

Process	$D_x/D_x$	$D_y/D_y$
MT	0.74	0.77
CT	0.69	0.68
EMCT	0.47	0.49

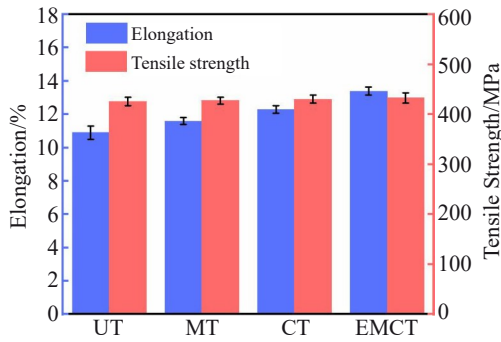


Fig.5 Tensile strength and elongation of original samples and samples treated with electromagnetic fields

improvement effect is the most significant when the electric field and magnetic field are coupled.

The fracture morphologies of the tensile sample are shown in Fig.6. The continuous dimples with different sizes in the fractures of all samples indicate a ductile fracture mode of the samples and significant plastic deformation occurs before fracture. Fig.6a shows the sample in its original state. The

dimples are coarse and unevenly distributed in the fracture, and the second small particles exist at the bottom of the dimples. This is consistent with the low elongation of the original sample in the tensile test. After a single magnetic field treatment, more particles of the second phase are still visible at the port (Fig.6b). The element analysis results in Fig.7 show that the components of the second phase are mainly Al, Mn and Cu, and the content of Mg is very little. After electric field treatment, smaller elliptical dimples appear in the fracture, and the second phase particles are significantly reduced (Fig.6c). Compared with the aluminum matrix, the hard second phase (such as  $\text{CuAl}_2$  and  $\text{Al}_2\text{MgCu}$ ) is more brittle and easier to become the fracture origin in the process of plastic deformation. After the sample is treated with electromagnetic coupling (Fig. 6d), the dimples in the fracture are more uniform and fine, distributed in contiguous pieces, and no obvious second phase particles are observed, indicating that the plasticity of the material is improved at this time, and thus, greater elongation is tested in the tensile experiment. According to the analysis, when the current passes through the sample, the Joule effect leads to an increase in heat

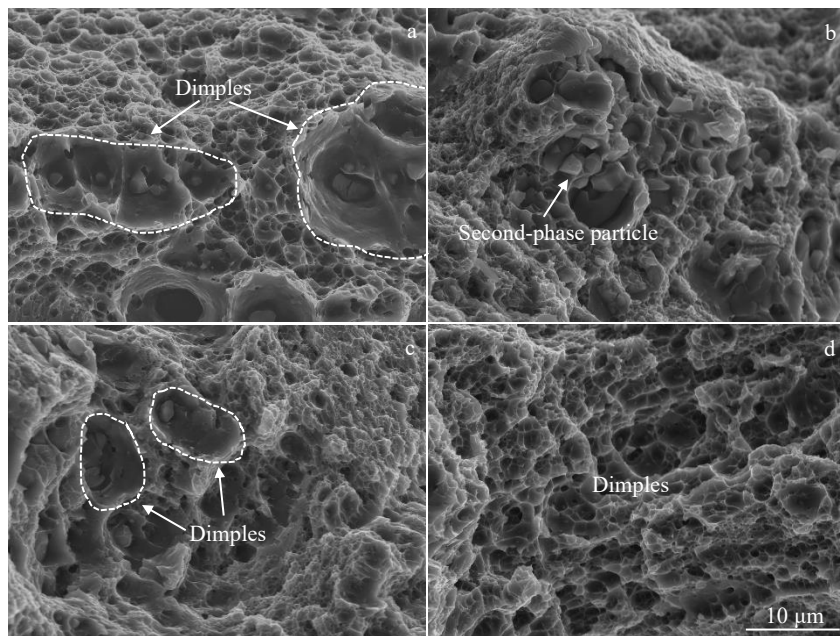


Fig.6 Tensile fracture morphologies of the samples UT (a), MT (b), CT (c), and EMCT (d)

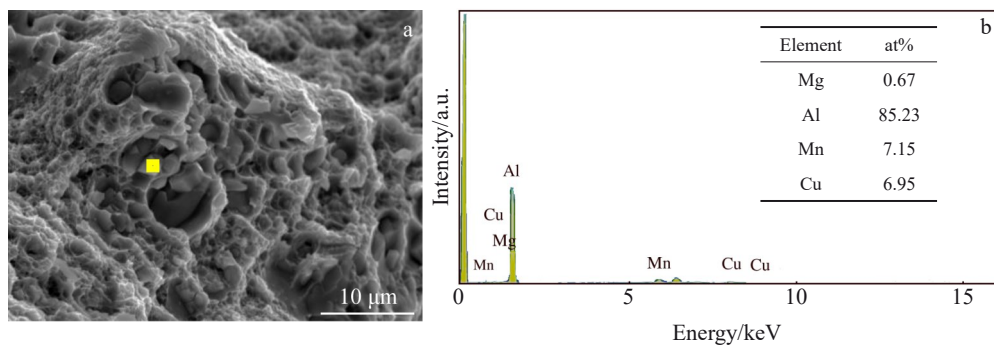


Fig.7 Fracture morphology (a) and EDS results (b) of second phase particle in tensile fracture

accumulation temperature in a short time, which promotes the second phase to dissolve into the matrix<sup>[23]</sup>.

### 2.3 Electrical conductivity

The electrometer was used to measure the room temperature resistance of the sample in different processes, and then the resistivity was calculated. The results are shown in Fig. 8. The room temperature resistivity of the original sample is  $2.939 \times 10^{-8} \Omega \cdot m$ . The resistivity is slightly reduced after the sample was treated with a single magnetic field or electric field. After the electromagnetic coupling treatment, the resistivity of the sample is  $2.795 \times 10^{-8} \Omega \cdot m$ , reduced by 4.9%. Studies have shown that the state of defects such as dislocation in the alloy will affect the electrical and thermal properties<sup>[24]</sup>. The experimental results show that the electromagnetic coupling treatment is helpful to reduce the resistivity of 2A02 aluminum alloy and to improve its conductivity at room temperature. The dislocation density within the sample decreases during the electromagnetic coupling treatment, and the dislocation tends to be in a short-range ordered state<sup>[24]</sup>. Therefore, the scattering effect of the dislocation on electrons decreases, and thus the resistivity of the material decreases<sup>[25]</sup>.

### 2.4 EBSD analysis

The process of residual stress reduction is essentially the result of accumulation of various inelastic deformation occurring inside the material. Quasi-in-situ EBSD analysis

was performed for the samples treated with electromagnetic coupling. Kernal average misorientation (KAM) distribution is a method to characterize local dislocation characters, which is usually used to illustrate the local strain distribution in crystalline materials. At the same time, it can also reflect the local dislocation density in materials. The larger the KAM value, the higher the local dislocation density. Fig. 9a and 9b show KAM distribution before and after electromagnetic coupling treatment in the same region of the same sample, respectively. As can be seen from Fig. 9a, prior to the electromagnetic coupling treatment, there is a distinct KAM highlighting region, distributed intensively within the crystal, as indicated by the arrow. The results show that during the forging process, the material deforms along the pressure direction, resulting in a large number of dislocation and local strain, which mainly accumulate in the grain, and a small amount of them distribute in the grain boundary. Thus the macro performance is high residual stress state of the forging.

After the electromagnetic coupling treatment, KAM distribution is more uniform in the whole field of view, showing a point distribution at the grain boundary. The highlighted regions of the concentrated contiguous segments disappear, and the bright regions exist only in a few smaller grains. This indicates that the local strain accumulation in the material is reduced and the dislocation density is homogenized after the electromagnetic coupling treatment.

In the process of electromagnetic coupling treatment, the magnetic field can provide guidance for the depinning of dislocation, and the electric field can provide energy for the movement of dislocation through conduction electrons as the driving force<sup>[26]</sup>. When the energy accumulation exceeds the threshold, the dislocation begins to decompose and slip, and the dislocations with equal Burgers vector size and opposite direction meet and annihilate, and the unannihilated dislocation will continue to slip, and stop until the resistance is greater than the driving force. In this process, a large number of dislocations annihilate and local strain accumulation decreases, thus achieving macro-stress relaxation and plasticity improvement. Eq. (2) is used to

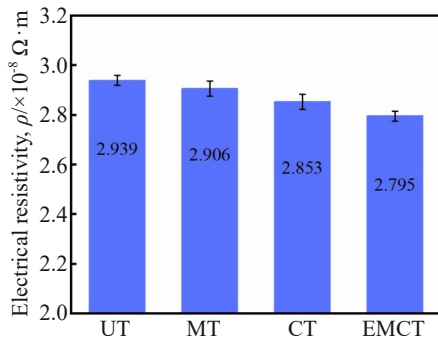


Fig.8 Room temperature resistivity of different samples

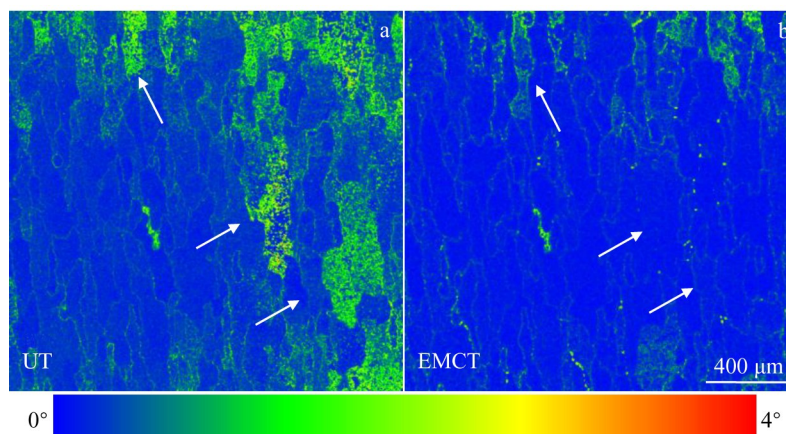


Fig.9 KAM distributions of samples before (a) and after (b) EMCT

calculate the geometric dislocation density<sup>[27]</sup>:

$$\rho^{\text{GND}} = 2\text{KAM}_{\text{ave}}/\mu b \quad (2)$$

where  $\rho^{\text{GND}}$  represents the geometric dislocation density,  $\mu$  represents the test step size,  $b$  represents the Burgers vector length, and  $\text{KAM}_{\text{ave}}$  represents the average KAM value of the test area, which can be calculated by Eq.(3):

$$\text{KAM}_{\text{ave}} = \exp\left[\frac{1}{N} \sum_1^i \ln \text{KAM}_{L,i}\right] \quad (3)$$

where  $\text{KAM}_{L,i}$  represents the local KAM value at point  $i$ , and  $N$  represents the number of test points in the region. The final calculation result of the geometrically required dislocation density of the same sample is as follows:  $9.77 \times 10^8 \text{ m}^{-2}$  before treatment and  $4.08 \times 10^8 \text{ m}^{-2}$  after treatment. In other words, the electromagnetic coupling treatment reduces the dislocation density of the material by about 58.2%, alleviates the microscopic strain, and thus achieves stress relaxation.

Fig. 10a and 10b shows the recrystallization of the same sample before and after electromagnetic coupling treatment in the same region, respectively. As can be seen from Fig. 10a, recrystallized grains and substructural grains are mainly in the original sample, accounting for 40.4% and 56.9%, respectively, while deformed grains is only 2.7%. This indicates that the forged deformation crystals have transformed into a large number of recrystallized and substructural grains after solution and aging treatments. After electromagnetic coupling treatment, the proportion of

recrystallized grains increases to 51.3%, the substructural grains decreases to 47.9%, and the deformed grains only remains 0.8%. In the process of sliding, the dislocation annihilates, which reduces the deformation energy of the material. In addition, driven by electron wind and magnetoplastic effects<sup>[28]</sup>, the kinetic energy of dislocation is enhanced, and the process of decomposition and slip is accelerated. The resulting high-density dislocation will generate more subgrains, and accelerate dynamic recrystallization by absorbing dislocation<sup>[29]</sup>. At the same time, the micro-zone thermal effect and thermal stress provided by the electromagnetic coupling treatment also prolong the recrystallization process, thus increasing the content of recrystallized grains.

Dislocation plugging in the grain and at grain boundaries causes stress concentration in this area. When the dislocation accumulates to a certain extent, the elastic stress field will force the dislocation to move, resulting in a change in the angle of the grain boundary. Fig. 11a and 11b show the change of grain boundary distribution in the same sample before and after electromagnetic coupling treatment. Small-angle grain boundary ( $<10^\circ$ ) is represented in red, while large angle grain boundary ( $>10^\circ$ ) is represented in black. As can be seen from Fig. 11, the samples in the original state have obviously contiguously small-angle grain boundaries. After electromagnetic coupling treatment, the content of small-angle

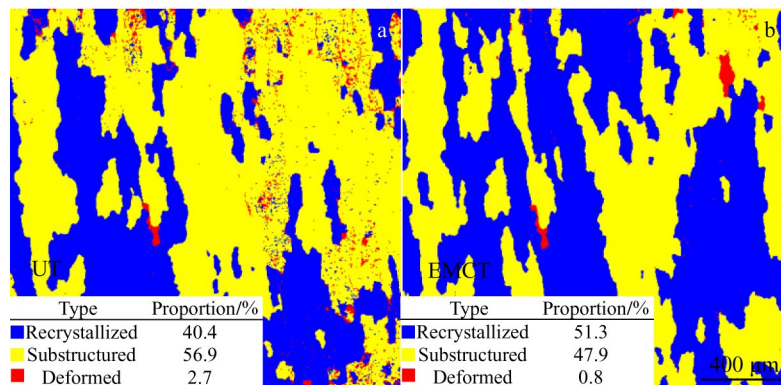


Fig.10 Recrystallization of samples before (a) and after (b) EMCT

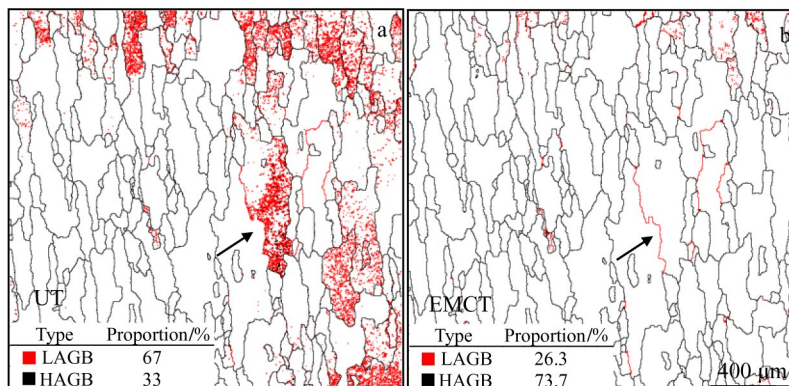


Fig.11 Grain boundary distribution of samples untreated (a) and after EMCT (b)

grain boundaries decreases from 67% to 26.3%, while the content of large-angle grain boundaries increases from 33% to 73.7%. Dislocation theory indicates that the small-angle grain boundary is the plugging area of dislocation, storing a large amount of the second type of internal stress<sup>[30]</sup>. Therefore, the significant reduction of small-angle grain boundary reflects the decrease in dislocation annihilation or dislocation density, which is consistent with the results observed by KAM. At the same time, the reduction in small-angle grain boundaries is accompanied by the release of the second type of internal stress, resulting in a macro-stress relaxation, which is consistent with the residual stress test results of the samples.

### 3 Conclusions

1) Electromagnetic field treatment can promote residual stress relaxation of 2A02 aluminum alloy blades, and the effect of electromagnetic coupling treatment is better than that of single electric or magnetic field treatment, which can reduce the overall stress level of blades by 53%.

2) The electromagnetic coupling treatment can induce the transformation from tensile stress to compressive stress state in some areas, which is helpful to restrain crack propagation and is beneficial to increase fatigue performance of blades.

3) The thermal effect of the current can promote the dissolution of the second phase, thus improving the plasticity of the material and increasing the elongation by 14.3%. The electromagnetic coupling treatment reduces the dislocation and the scattering effect of the dislocation on the electrons, so that the resistivity of the material is decreased by 4.9%.

4) The electromagnetic coupling treatment results in dislocation annihilation in the sample, the geometric dislocation density is decreased by 58.2%, the small-angle grain boundaries are greatly reduced, and the local strain accumulation is reduced, thus achieving the stress relaxation of blade forging.

### References

- Li E, Zhou J, Yang C et al. *Journal of Manufacturing Processes*[J], 2023, 92: 397
- Chen Z, Yue C, Xu Y et al. *Journal of Materials Processing Technology*[J], 2023, 314: 117 907
- Ju K, Duan C, Sun Y et al. *Journal of Materials Processing Technology*[J], 2022, 307: 117 664
- Qin Guohua, Lin Feng, Ye Haichao. *Rare Metal Materials and Engineering*[J], 2018, 47(11): 3400
- Yu B, Wang P, Song X et al. *International Journal of Pressure Vessels and Piping*[J], 2022, 200: 104 852
- Goviazin G G, Rittel D, Shirizly A. *Materials Science and Engineering A*[J], 2023, 873: 145 043
- Měsíček J, Cegan T, Ma Q et al. *Materials Science and Engineering A*[J], 2022, 855: 143 900
- Tang H, Gao C, Zhang Y et al. *Journal of Materials Science & Technology*[J], 2023, 139: 198
- Teimouri R, Skoczypiec S. *Journal of Manufacturing Processes*[J], 2022, 80: 116
- Huang G, Zhang Q, Zhang B et al. *Results in Physics*[J], 2021, 29: 104 659
- Lu A L, Tang F, Luo X J et al. *Journal of Materials Processing Technology*[J], 1998, 74(1): 259
- Cai Z P, Lin J A, Zhou L A et al. *Materials Science and Technology*[J], 2004, 20(12): 1563
- Song Y, Hua L. *Journal of Materials Science & Technology*[J], 2012, 28(9): 803
- Shao Q, Kang J, Xing Z et al. *Journal of Magnetism and Magnetic Materials*[J], 2019, 476: 218
- Zhang Y, Fang C, Huang Y et al. *Journal of Magnetism and Magnetic Materials*[J], 2021, 540: 168 327
- Yan M, Wang C, Luo T et al. *Acta Metallurgica Sinica*[J], 2021, 34(1): 45
- Xiang S, Zhang X. *Acta Metallurgica Sinica*[J], 2020, 33(2): 281
- Yuan M, Wang J, Wang M et al. *The International Journal of Advanced Manufacturing Technology*[J], 2020, 108(11–12): 3905
- Geng H, Xu X, Cao Q et al. *The International Journal of Advanced Manufacturing Technology*[J], 2022, 120(7–8): 5057
- Zhong F, Wang J, Zhang Q et al. *The International Journal of Advanced Manufacturing Technology*[J], 2022, 121(7–8): 4757
- Sun Qian, Sun Xiangyang, Song Yanli et al. *The Chinese Journal of Nonferrous Metals*[J], 2023, 33(3): 752
- Cong Jiahui, Wang Lei, Xu Yongzhen et al. *Rare Metal Materials and Engineering*[J], 2022, 51(1): 113
- Xu X, Zhao Y, Wang X et al. *Materials Science and Engineering A*[J], 2016, 654: 278
- Lang C I, Shaw M P. *Materials Science & Engineering A*[J], 1993, 164(1–2): 180
- Raeisnia B, Poole W J. *Materials Science Forum*[J], 2006, 519–521: 1391
- Cai Z, Huang X. *Materials Science and Engineering A*[J], 2011, 528(19–20): 6287
- Li Zhenliang, Tian Dongkuo. *Rare Metal Materials and Engineering*[J], 2021, 50(2): 639
- Yuan M, Wang J, Wang L et al. *Ceramics International*[J], 2021, 47(3): 3747
- Wang Q, He X, Deng Y et al. *Journal of Materials Research and Technology*[J], 2021, 12: 2348
- Robinson J S, Hossain S, Truman C E et al. *Materials Science and Engineering A*[J], 2010, 527(10–11): 2603

## 电磁耦合能作用下2A02叶片锻件的残余应力松弛

曾波<sup>1,2</sup>, 谢志强<sup>3</sup>, 李强<sup>1,2</sup>, 王杰<sup>1,2</sup>, 黄坤兰<sup>1,2</sup>, 于航<sup>1,2</sup>

(1. 四川大学机械工程学院, 四川 成都 610065)

(2. 宜宾四川大学产业技术研究院, 四川 宜宾 644005)

(3. 中国航发成都发动机有限公司, 四川 成都 610599)

**摘要:** 针对航空大尺寸薄壁件因残余应力释放导致加工变形的行业问题, 提出了一种电磁耦合处理的新型材料处理方法, 并将其应用于调控压气机2A02铝合金叶片锻件的残余应力。研究了电、磁场工艺对锻件残余应力和力学性能的影响; 并对材料组织开展准原位EBSD分析。结果表明, 相较于单一物理场, 电磁耦合处理对残余应力的松弛效果最显著, 在磁场强度为1.5 T、电场强度为750 V/m时, 叶片锻件残余应力最大降幅为53%。电磁耦合处理可以在不损害强度的情况下, 改善铝合金塑性, 在上述电磁场参数下, 其伸长率提高14.3%, 电阻下降4.9%。EBSD准原位分析表明, 电磁耦合处理后, 锻件的几何位错密度降低58.2%, 小角度晶界减少, 塞积的位错分散、湮灭, 局部应变降低, 宏观应力松弛。

**关键词:** 铝合金锻件; 残余应力; 电磁耦合处理; 位错湮灭

作者简介: 曾波, 男, 1995年生, 博士生, 四川大学机械工程学院, 四川 成都 610065, E-mail: zengb1995@163.com